Ultrathin AlO_x-TiO_y Film Formation by Controlled Oxidation of Titanium Deposited on Polycrystalline Aluminum Surfaces

A. Arranz and C. Palacio*

Departamento de Física Aplicada, Facultad de Ciencias, C-XII, Universidad, Autónoma de Madrid, Cantoblanco, 28049-Madrid, Spain

Received: January 18, 2002; In Final Form: May 30, 2002

The interaction of oxygen with titanium deposited on polycrystalline aluminum surfaces has been studied at room temperature and low oxygen pressures, using AES, XPS, and ARXPS. The growth of titanium on the aluminum surfaces occurs in two stages: formation of a uniform $TiAl_x$ layer up to ∼4 monolayers (ML), followed by the formation of metallic titanium islands 10 ML thick that grow over the $TiAl_x$ layer previously formed. The oxidation of Ti/Al interfaces shows the formation of an aluminum intermediate oxidation state, Al^{2+}, in addition to Al^{3+}, which is attributed to the formation of Al−O−Ti cross-linking bonds at the interface between an outer aluminum oxide-Ti^{4+} mixed layer and a film beneath it composed by a mixture of titanium suboxides. The Al_2O_3 concentration in the oxide film decreases as the Ti deposition time previous to oxidation increases, as a consequence of the thickening of the $TiAl_x$ layer up to 4 ML in the first stage of Ti growth and subsequent formation of metallic Ti islands in the second stage. The Al^{2+} concentration reaches a maximum at the end of the first stage of Ti growth, decreasing afterward because of metallic Ti islands oxidation. The analysis of the Ti 2p band shows Ti oxidation for Ti/Al interfaces of both the first and second stage of titanium growth. However, for Ti/Al interfaces of the first stage, the ratio between Ti^{4+} and titanium suboxides, the lack of the oxygen signal characteristic of pure Ti oxidation, and the formation of an oxygen species in the high binding energy side of the O 1s band, related to the titanium oxidation of the $TiAl_x$ compound, suggest the formation of an aluminum titanate-like compound.

Introduction

Thin films of metal oxides at nanometer scale have been prepared during the oxidation of metal/metal interfaces.[1−7] In particular, the growth and characterization of ultrathin mixed oxide layers have attracted great attention because of the better catalytic, optical, dielectric, and mechanical properties of the mixed oxides in comparison with the single components.[8] For instance, nanosized $Al_2O_3-TiO_2$ mixed oxides are used as catalyst supports.[9] Likewise, it has been found an enhancement of the activity of TiO_2 species to several isomerization reactions by the addition of small amounts of Al_2O_3.[10,11] $Al_xTi_yO_z$ mixed oxide thin films of variable composition have been also proposed as dielectric of variable refraction index.[12,13] On the other hand, the surface oxide grown at room temperature on bulk Ti−Al alloys plays an important role in aeronautic and biotechnological applications, since it determines the corrosion resistance and bonding properties of the alloy.

The initial oxidation of Ti−Al bulk alloys has been studied by several authors, showing a complex pattern.[14−16] Mencer et al. have found that the oxidation process is controlled by temperature, oxygen pressure, the bulk alloy composition, and the formation free energies of the different oxides detected in the overlayers.[14] Geng et al. have observed an important influence of the "in situ" cleaning procedure on the oxidation behavior of the TiAl alloy.[15] Shanabarger has studied the initial oxidation of bulk Ti−Al alloys at room temperature as a function of the Al concentration in the alloy using Auger electron spectroscopy. He found that the initial oxygen adsorption rate decreases with increasing surface Al concentration.[16]

However, no studies on the oxidation of the bimetallic system formed at the Ti/Al interface have been performed. Therefore, the aim of this work is to use Auger electron spectroscopy (AES), X-ray photoelectron spectroscopy (XPS), and angle resolved X-ray photoelectron spectroscopy (ARXPS) to study the oxygen reactivity of the Ti/Al interface at room temperature. The formation of the Ti/Al interface during deposition of Ti on polycrystalline Al at room temperature has been characterized in a previous work.[17] The experimental results were consistent with a two-stage mechanism for the titanium growth. The first stage was characterized by the formation of a uniform layer ∼4 ML thick of $TiAl_x$ ($x = 1.5$), followed by the formation of metallic titanium islands with an average thickness of 10 ML which grow laterally.

Experimental Section

High-purity polycrystalline aluminum substrates (nominal composition 99.994% Al, 0.004% Si, 0.001% Fe, and 0.001% Cu) manufactured by Toyo Aluminum Co., Japan, were used throughout this work. They were degreased by successively boiling in carbon tetrachloride, acetone, and ethanol. Then the sample was introduced into the UHV chamber. The aluminum substrates were sputter-cleaned in situ with 3 keV Ar^+ until no impurities were detected by AES. To minimize the surface roughness attained after sputter cleaning, the ion current density was kept below 2 $\mu A/cm^2$. As measured by "ex-situ" atomic force microscopy, such a low current density develops small and uniform roughness that should not influence, from a qualitative point of view, the spectroscopic results.

* Corresponding author. Fax: ++34 91 3974949. E-mail: carlos.palacio@uam.es.

10.1021/jp025532b CCC: $22.00
Published on Web 08/21/2002

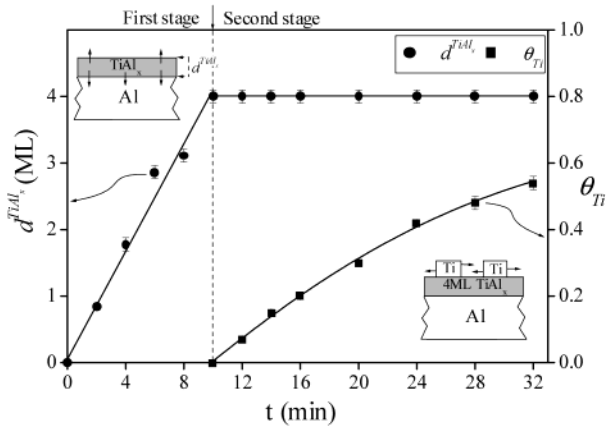

Figure 1. Thickness of the $TiAl_x$ layer, d^{TiAl_x}, and coverage of Ti islands, θ_{Ti}, as a function of Ti deposition time on Al substrates. A schematic model of the Ti/Al interface formation is also given. The first stage of growth (top left panel) is characterized by the formation of a uniform $TiAl_x$ layer up to a thickness of ~4 ML for $t = 10$ min. The second stage (bottom right panel) is characterized by the formation and growth of pure titanium islands over the $TiAl_x$ layer previously formed.

Experimental details for titanium deposition and for AES and XPS characterization have been given in detail elsewhere[17] and will only be summarized here. Titanium was deposited by sublimation of a directly heated filament of 99.6% purity onto the Al substrates at room temperature. The titanium deposition rate was $\sim 2.5 \times 10^{14}$ atoms·cm^{-2}·min^{-1}. Auger spectra were measured in the derivative mode using a cylindrical mirror analyzer (CMA) with a nominal resolution of 0.25%. A modulation voltage of 2 V_{p-p} was supplied to the CMA. A constant primary electron beam current density of 1×10^{-3}A/cm^2 at 3 keV primary beam energy was used. XPS data were recorded using a hemispherical analyzer (SPECS EA-10 Plus). The pass energy was 15 eV giving a constant resolution of 0.9 eV. A twin anode (Mg and Al) X-ray source was operated at a constant power of 300 W, using Mg Kα (1253.4 eV) radiation. The oxidation was carried out at room temperature. For the oxidation experiments, oxygen 5 N quality, was introduced into the spectrometer chamber at a controlled partial pressure in the $10^{-8}-10^{-5}$ Torr range. The partial pressure of oxygen and the purity of the gas were controlled by means of a quadrupole mass analyzer.

Results

The characterization of the interface formed during the deposition of titanium on polycrystalline Al substrates at room temperature has been carried out in a previous work using AES−FA, XPS, and ARXPS.[17] In that work, a two-stage mechanism for titanium growth was proposed: a first stage (up to 10 min Ti deposition time) characterized by the formation of a uniform $TiAl_x$ ($x = 1.5$) layer up to ~4 monolayers (ML), followed by the formation of 10 ML thick metallic titanium islands which grow laterally over the $TiAl_x$ layer previously formed. Metallic titanium was only detected on the surface during the second stage. During the first stage, deposited titanium reacts with the aluminum substrate to form the intermetallic compound, $TiAl_x$. Figure 1 summarizes such a model, showing the thickness of the $TiAl_x$ layer, d^{TiAl_x}, and the coverage of the metallic titanium islands, ϑ_{Ti}, as a function of titanium deposition time. A schematic diagram of the model for the Ti/Al interface formation is also given in Figure 1. Similar two-stage mechanisms have been also found during iron and nickel deposition on polycrystalline Al substrates.[18,19] However, in contrast with the Ti/Al interface, the first stage was characterized in those metals by the formation of Fe−Al or Ni−Al islands, respectively. This difference should be attributed to a higher mobility and reactivity of deposited titanium, in comparison with iron and nickel, which are responsible for the formation of a uniform $TiAl_x$ layer instead of islands.

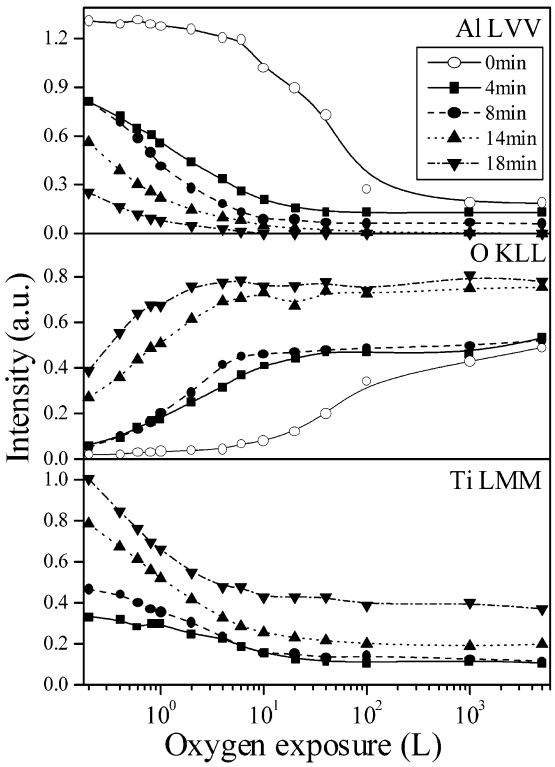

Figure 2. Evolution of the Al LVV, O KLL, and Ti LMM Auger intensities as a function of the oxygen exposure for several Ti deposition times.

Different Ti/Al interfaces corresponding to both the first stage ($t \leq 10$ min) and the second stage ($t > 10$ min) of titanium growth on Al substrates have been oxidized at room temperature. The oxygen exposure was increased up to 5000 L (1 L $\equiv 10^{-6}$ Torr·s). To characterize the thin oxide film formed, the Al LVV, Ti LMM, and O KLL Auger transitions as well as the Al 2p, O 1s, and Ti 2p XPS bands have been measured for different titanium deposition times and subsequent oxygen exposure.

Figure 2 shows the evolution of the Al LVV, O KLL, and Ti LMM Auger intensities as a function of the oxygen exposure for different Ti deposition times. For $t > 0$ min, a strong attenuation of the aluminum and titanium Auger intensities, along with a fast increase of the oxygen intensity, can be observed in the range 0.2−4 L. The evolution of the Auger signals depends on the Ti deposition time, in such a way that the value at which signal saturation is reached shifts to lower oxygen exposures as the Ti deposition time increases. In addition, the oxygen intensity at saturation also increases with deposition time. As pointed out by Valeri et al.[20] in their study of Ni silicides, this catalytic effect of deposited Ti on the reactivity of the substrate should be attributed to its ability to break the O_2 molecule exposing aluminum to atomic oxygen which is much more reactive. Shanabarger[16] has studied by AES the initial oxidation of bulk Ti−Al alloys at room temperature as a function of the Al concentration of the alloy. He found an initial oxygen adsorption rate that increases with increasing surface Ti concentration in the alloy, in good agreement with the behavior observed in Figure 2. To explain this result,

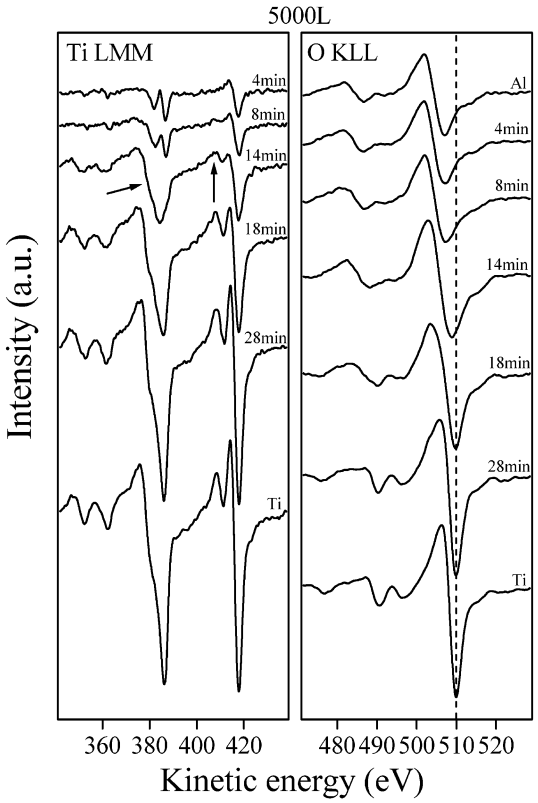

Figure 3. Derivative Ti LMM and O KLL Auger spectra of the 5000 L oxide films measured for different Ti/Al interfaces.

Shanabarger has suggested that oxygen dissociative adsorption occurs primarily at the Ti surface atoms of the Ti−Al alloy and not at the Al atoms.[16]

Figure 3 shows the Ti LMM and O KLL Auger transitions of 5000 L oxide films measured for different Ti/Al interfaces. The AES spectra for Ti exhibit important changes associated with titanium oxidation (indicated by arrows) when Ti/Al interfaces corresponding to the second stage ($t > 10$ min) are exposed to oxygen. For the first stage ($t \leq 10$ min), changes are subtler than for the second stage and consist of variations of the relative intensities and broadening of the Auger peaks, as compared with the unexposed Ti/Al interface (not shown in the figure). On the other hand, the O KLL peaks show a chemical shift and shape changes as the titanium content increases. For Ti deposition times ≥28 min, the oxygen Auger spectrum is similar to that measured for an oxygen exposed Ti substrate, labeled Ti in Figure 3, therefore indicating that the oxidation is dominated by the oxidation of the metallic titanium islands.

The Al 2p, O 1s, and Ti 2p XPS bands were measured for different Ti/Al interfaces and oxygen exposures up to 5000 L. Measured spectra of aluminum, oxygen, and titanium, after background subtraction based on a modified Shirley method,[21] are shown in Figure 4a−4c, respectively. Although oxygen exposures were carried out in the range 0−5000 L, for simplicity only results corresponding to an oxygen exposure of 5000 L are given in Figure 4a−4c. Upon increasing oxygen exposure (not shown), a broad shoulder appears on the high binding energy (BE) side of the Al 2p band. Also, an attenuation of the metallic Al 2p band is observed. Results corresponding to an exposure of 5000 L show that the position of the Al 2p shoulder shifts to the lower BE as the titanium content increases. Figure 4b shows the measured spectra of the O 1s band for different titanium deposition times. The band shifts from ∼532 eV for

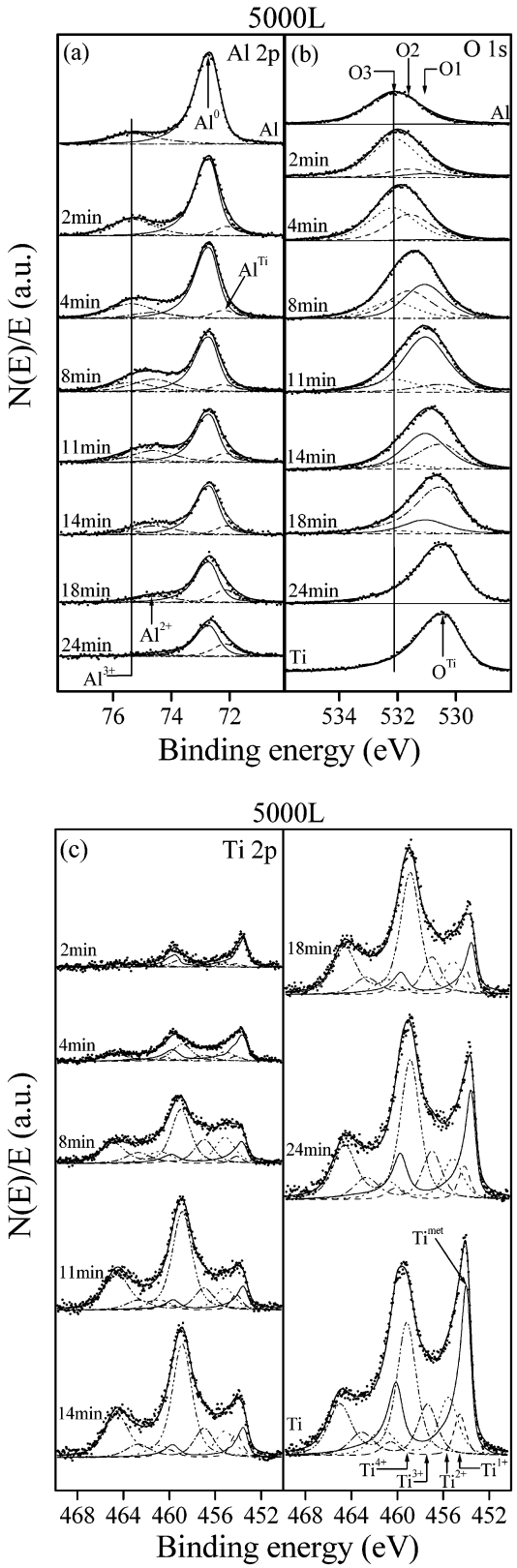

Figure 4. XPS spectra of the 5000 L oxide films measured for different Ti/Al interfaces. (a) Al 2p band; (b) O 1s band; (c) Ti 2p band.

the Al substrate to ∼530.4 eV for pure Ti, indicating the presence of at least four components. Also, an attenuation of the metallic Ti 2p band is observed along with the apparition of new peaks in the high BE side of the Ti 2p band that are associated with the oxidation of titanium. For deposition times corresponding to the first stage ($t \leq 10$ min), the oxidation of titanium is clearly observed in the Ti 2p XPS spectra, but the

TABLE 1: Parameters of the Synthetic Bands Ti^{met}, Ti^{1+}, Ti^{2+}, Ti^{3+}, and Ti^{4+} Used for Deconvolution of Ti 2p Spectra

band	E_o (eV)	*sos* (eV)	$w_{3/2}$ (eV)	$w_{1/2}$ (eV)	*R*
Ti^{met}	453.6	6.1	1.2	1.8	2.0
Ti^{1+}	454.1−454.2	6.0	1.4	2.0	2.0
Ti^{2+}	455.1−455.2	5.7	2.0	2.5	1.9
Ti^{3+}	456.9−457.0	5.7	2.0	2.5	1.9
Ti^{4+}	458.8−458.9	5.7−5.8	2.0	2.4	2.0

intensity of the new peaks at higher BE, associated with Ti oxidation, is smaller than for $t > 10$ min. This would explain the moderate changes observed in the Ti LMM AES spectra of Figure 3 for $t \leq 10$ min.

To determine the bands associated with the different Al, Ti, and O species by peak deconvolution, synthetic spectra and a least-squares optimization were used. Four synthetic bands have been used to reproduce the Al 2p spectra in the whole range of titanium deposition times and oxygen exposures. An asymmetrical Gaussian−Lorentzian (GL) function, Al^0, associated with metallic aluminum; a symmetrical GL function, Al^{Ti}, attributed to the intermetallic compound $TiAl_x$; and two symmetrical GL functions, Al^{2+} and Al^{3+}, associated with 2+ and 3+ Al oxidation states, respectively. For Ti/Al interfaces of the first stage, Al^{2+} species are also present for exposures below 4 L and therefore can be also related to chemisorbed oxygen in this range of oxygen exposures. In addition to 2+ and 3+ Al oxidation states, Al 1+ oxidation state has been also detected in the oxide films formed during the oxidation of Fe/Al and Ni/Al interfaces.[6,7] However, the use of a fifth band, Al^{1+}, associated with this oxidation state is not necessary to reproduce the whole data set for the oxidation of the Ti/Al interface. For the oxidation of Fe/Al and Ni/Al interfaces during the first stage of deposition, that is, without "free" metallic Fe or Ni on the surface, no iron or nickel oxide was formed.[6,7] Fe and Ni 2p XPS bands only showed small changes that were attributed to Fe or Ni atoms in an Al depleted layer at the oxide−substrate interface, being Al^{1+} and Al^{2+} related to Fe/Ni−Al−O cross-linking bonds at the interface.[6,7] However, for the Ti/Al interface, the lower Al oxidation state, Al^{1+}, is not formed, suggesting either the formation of a lower number of Ti−O−Al cross-linking bonds or a different configuration of the Ti−O−Al network at the interface, as a consequence of the oxidation of titanium in the $TiAl_x$ compound.

Four components are needed to reproduce the O 1s band in the same range of titanium deposition times and oxygen exposures. The synthetic spectra related to these components are three symmetrical GL bands, O1, O2, and O3, and an asymmetrical GL band, O^{Ti}. The reference bands O3 and O^{Ti}, associated with Al_2O_3 and titanium oxide, respectively, were obtained from the measured O 1s spectra of the 5000 L oxygen exposed clean aluminum and titanium substrates, respectively.

For the Ti 2p band, five components, Ti^{met}, Ti^{1+}, Ti^{2+}, Ti^{3+}, and Ti^{4+}, attributed to metallic titanium, and 1+, 2+, 3+, and 4+ titanium oxidation states, respectively, have been used. In a first step, the synthetic doublet for the Ti 2p band of the clean Ti/Al interface, Ti^{met}, was obtained by a least-squares procedure using the Ti 2p measured spectra of the clean Ti/Al interface as reference. The corresponding synthetic doublet is formed by two asymmetrical GL functions, and the parameters defining the synthetic doublet are given in Table 1. The Ti $2p_{3/2}$ binding energy, E_o, the Ti 2p spin−orbit splitting, *sos*, the full width at half-maximum of the Ti $2p_{3/2}$ and Ti $2p_{1/2}$ peaks of the doublet, $w_{3/2}$ and $w_{1/2}$, and the Ti $2p_{3/2}/2p_{1/2}$ area ratio, *R*, are in good agreement with experimental values reported in the literature for metallic Ti.[17] It is important to observe $w_{1/2} > w_{3/2}$ in agreement with previous theoretical and experimental results found for 3d transition metals.[22,23] This difference has been attributed to the decrease in the Coster−Kronig−Auger decay with increasing angular-momentum quantum number. Furthermore, $w_{1/2} - w_{3/2}$ is a measure of the $L_2L_3M_{4,5}$ Coster−Kronig transition rate.[22] In addition, the experimental Ti $2p_{3/2}/2p_{1/2}$ area ratio, *R*, is in good agreement with the theoretical value.[24]

In a second step, the analytical shape of the Ti^{1+}, Ti^{2+}, Ti^{3+}, and Ti^{4+} components was found using a trial and error procedure involving all the measured spectra, that is, 120. The Ti $2p_{3/2,1/2}$ doublet of every component has been simulated by two symmetrical GL functions. In a first attempt, parameters *sos*, $w_{3/2}$, and $w_{1/2}$ were taken to be equal for all the Ti oxidation states. Initial estimations for E_o, *sos*, $w_{3/2}$, $w_{1/2}$, and *R*, were taken from the values found for a TiO_2 reference sample measured under the same experimental conditions. In all cases, the parameter *R* takes values very close to the theoretical value.[24] However, no acceptable agreement between the curve fit and experimental results was obtained, mainly in the low oxygen exposure regime in which the Ti^{1+} component is dominant. The only possibility to have good fittings was allowing the parameters *sos*, $w_{3/2}$, and $w_{1/2}$ of Ti^{1+} component to take values between the metallic Ti ones and those corresponding to Ti^{2+}, Ti^{3+}, and Ti^{4+} components. After the trial and error procedure, the best parameters defining the Ti^{met}, Ti^{1+}, Ti^{2+}, Ti^{3+}, and Ti^{4+} synthetic doublets are those given in Table 1. As it can be observed, these parameters are in good agreement with those reported in the literature.[25,26] Although Ti^{1+} states have been already reported,[25,27] the only information available about them is the Ti^{1+} $2p_{3/2}$ binding energy that is located ~4.2 eV below that of Ti^{4+} $2p_{3/2}$.[25] The values defining the Ti^{1+} synthetic component (see Table 1) point to a possible metallic character of this species. Finally, in the final least-squares fit of Figure 4c, between the experimental Ti 2p spectra and the synthetic bands, peak heights were the only adjustable parameters.

Figure 5 shows (a) the evolution of the Al, O, and Ti XPS peak areas as a function of the oxygen exposure, for a titanium deposition time of 4 min, that corresponds to the first stage of the Ti/Al interface formation. In addition, in (b) the evolution of the same XPS signals as a function of the oxygen exposure for a Ti deposition time of 18 min, corresponding to the second stage of titanium deposition, is also shown. The intensities *I* (peak areas) are normalized to the corresponding sensitivity factors, *S*.[24] On the other hand, Figure 6 shows the evolution of Al, O, and Ti XPS signals as a function of the titanium deposition time for an oxygen exposure of 5000 L. Figures 5 and 6 clearly show that the composition of the thin oxide film formed depends on both the titanium deposition time and oxygen exposure. To obtain further information on the in-depth distribution of the different Al and Ti species, ARXPS measurements were carried out for all Ti/Al interfaces exposed to 5000 L. Figure 7 shows different peak area ratios between Al and Ti species as a function of the takeoff angle relative to the surface normal for (a) $t = 4$ min (first stage of Ti deposition) and (b) $t = 18$ min (second stage). In this figure, Al^{ox} and Ti^{subox} correspond to the $Al^{2+} + Al^{3+}$ and $Ti^{1+} + Ti^{2+} + Ti^{3+}$ contributions, respectively. As discussed below, a comparative analysis of the evolution of these ratios will give qualitative information on the in-depth composition of the oxide film formed.

Discussion

According to the signal evolutions of Figures 5 and 6, the O1 species should be related to the formation of 2+ Al

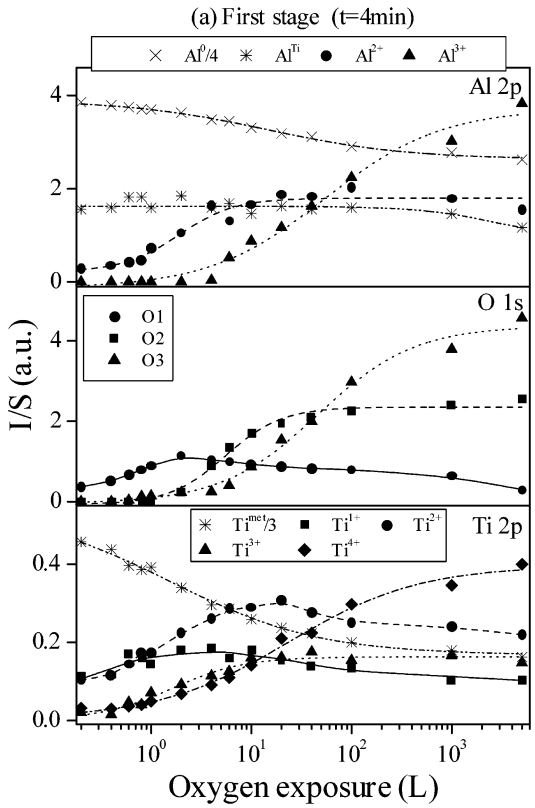

Figure 5. Normalized intensities (normalization is explained in the text) as a function of oxygen exposure of Al 2p, O 1s, and Ti 2p signals for (a) a Ti/Al interface corresponding to the first stage of titanium deposition on aluminum; (b) a Ti/Al interface corresponding to the second stage of deposition.

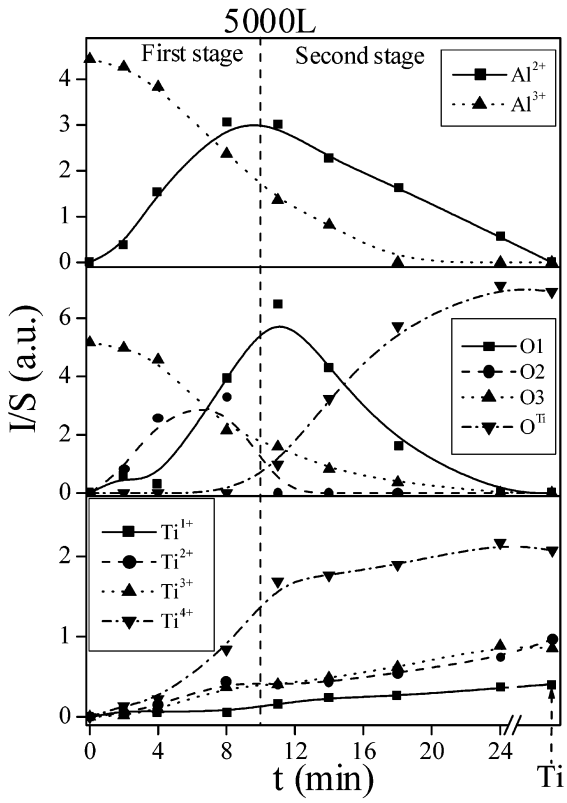

Figure 6. Normalized intensities as a function of the titanium deposition time of Al 2p, O 1s, and Ti 2p signals measured for the 5000 L oxide films.

intermediate oxidation state in good agreement with the results found in the oxidation of Fe/Al and Ni/Al interfaces.[6,7] The comparison of the results corresponding to both stages of Ti growth (Figures 5 and 6) shows that the O2 species is only observed for $t \leq 10$ min, that is, during the first stage of Ti deposition. In addition to that, it is important to indicate the following points. First, the study of the evolution of the O 1s spectrum during the oxidation of a high-purity Ti substrate (not presented in this work) has shown that two different symmetric GL, $O1^{Ti}$ and $O2^{Ti}$ at 531.5 and 530.4 eV, respectively, should be used to reproduce the O 1s spectrum for all oxygen exposures, being attributed to $Ti^{1+} - Ti^{2+}$ and $Ti^{3+} - Ti^{4+}$, respectively.[28] For oxygen exposures above 100 L, the combination of these two components gives an asymmetric shape for the O 1s spectrum similar to that observed in the spectrum labeled O^{Ti} in Figure 4b. Because of the complete overlapping of $O1^{Ti}$ and O2 bands, only O2 band has been used in the deconvolution procedure presented here, whereas a unique asymmetric band, O^{Ti}, has been used to account for $O1^{Ti}$ and $O2^{Ti}$ bands at 5000 L. Second, Ti^{1+}, Ti^{2+}, Ti^{3+}, and Ti^{4+} species are observed for all deposition times, even for $t \leq 10$ min, when all deposited Ti has reacted with aluminum to form a $TiAl_x$ layer. However, the O^{Ti} species, associated with titanium oxidation, only is observed for $t > 10$ min, when free metallic titanium is present at the surface. Finally, the Al^{1+} species is not observed at all. Therefore, O2 species seems to be related to the different titanium oxidation states which appear during the oxidation of Ti/Al interfaces formed during the first stage, as a consequence of the Ti oxidation of the $TiAl_x$ compound. On the other hand, for the oxidation of Ti/Al interfaces of the second stage, that is, when free metallic titanium is present at the surface, O2 species disappears and the titanium oxidation is expressed by the O^{Ti} species, as can be observed in Figure 6. The lack of O^{Ti} signal for $t \leq 10$ min and the presence of the O2 species for $t \leq 10$ min, suggest the formation of a Ti−Al mixed oxide similar to aluminum titanate, Al_2TiO_5,[12,29] during the oxidation of Ti/Al interfaces of the first stage. Bulk

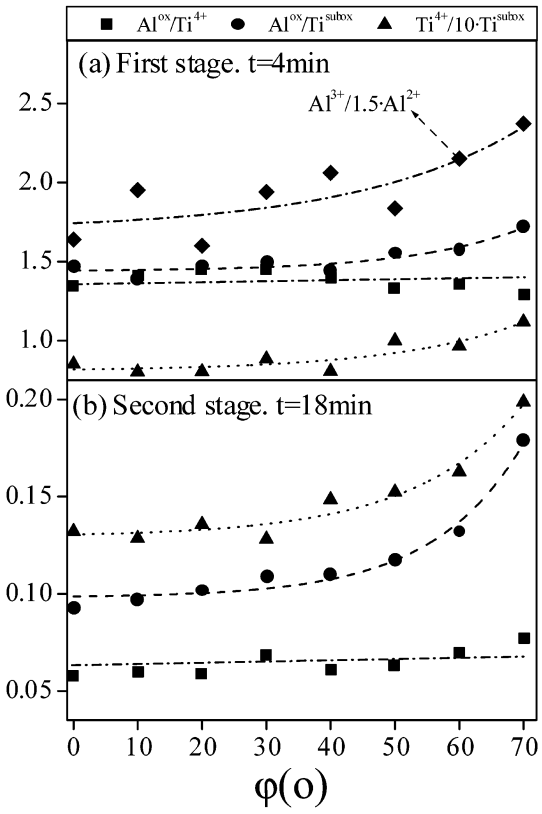

Figure 7. Variations of different XPS peak area ratios as a function of takeoff angle relative to the surface normal for a 5000 L oxide film grown on (a) an interface corresponding to the first stage of deposition ($t = 4$ min); (b) an interface corresponding to the second stage ($t = 18$ min).

thermodynamic data predicts that the formation of Al_2TiO_5 from Al_2O_3 and TiO_2 is an endothermic reaction below 1280 °C. Moreover, the growth of aluminum titanate during the formation of Ti/Al_2O_3 and Al/TiO_2 interfaces at room temperature has been suggested, as a consequence of the charge transfer between the deposited metal and the oxide substrate.[29,30]

Figure 5a and 5b suggests that titanium oxidizes stepwise with the initial formation of Ti^{1+} and Ti^{2+} species. The Ti^{1+} signal reaches a maximum at ~1−2 L decreasing above this exposure, whereas Ti^{2+} reaches a maximum at higher oxygen exposures (~20 L) decreasing slightly thereafter as a consequence of the formation of Ti^{3+} and Ti^{4+} species. The evolution of Ti^{3+} and Ti^{4+} species as a function of oxygen exposure shows sigmoidal shapes, reaching saturation for oxygen exposures above 100 L. The point at which Ti^{2+}, Ti^{3+}, and Ti^{4+} species reach the saturation shifts to lower oxygen exposures with increasing Ti deposition time, in agreement with the behavior observed for the Auger intensities of Figure 2. For $t \geq 18$ min, the evolution observed for the different Ti oxidation states as a function of the oxygen exposure is similar to that observed for a clean Ti substrate,[28] therefore indicating that the oxidation kinetics is controlled by the oxidation of the metallic titanium islands. However, for $t \leq 10$ min and saturation conditions, the ratio $Ti^{4+}/(Ti^{1+} + Ti^{2+} + Ti^{3+})$ decreases. This decrease is associated with the formation of the O2 species as well as with the formation of Al^{2+} and O1 species. According to thermodynamic data, the oxidation of Al accompanied by the reduction of Ti species is always favorable.[14] On the other hand, for $t >$ 10 min, the O2 species completely disappears, the Al^{2+} and O1 signals decrease as the O^{Ti} signal increases, and the $Ti^{4+}/(Ti^{1+} + Ti^{2+} + Ti^{3+})$ ratio tends to the value observed for pure Ti.

Sigmoidal shapes of the kinetic curves, similar to those of Figure 5a and 5b, have been also detected during the first stages of oxidation for pure Al,[31] Ti[28], and for the Fe/Al and Ni/Al systems.[6,7] This behavior is commonly explained by using an oxidation model that involves chemisorption of oxygen, oxide islands nucleation and growth until coalescence, and thickening of the oxide film.

As observed in Figure 5a and 5b, not only Al^{3+} (Al_2O_3) but also Al^{2+} is formed with increasing oxygen exposures. Moreover, Figure 6 shows that the signals Al^{3+} and O3 decrease with increasing titanium deposition time, and Al^{2+} and O1 signals show a maximum at ~10 min, decreasing above this Ti deposition time. Such a behavior can be explained considering that the substrate consists of a $TiAl_x$ layer for $t \leq 10$ min and of a double layer, metallic titanium islands on the $TiAl_x$ layer, for $t > 10$ min. The oxidation behavior shown in Figure 6 provides a nice confirmation of the transition in the Ti growth mode at $t = 10$ min.[17]

The shift to lower BE in the nonmetallic part of the Al 2p band (see Figure 4a) may arise from a decrease in the positive charge on Al atoms in the Al^{2+} intermediate oxidation state as a consequence of the formation of Ti−O−Al cross-linking bonds. This interpretation is also supported by the presence of O1 band at intermediate BE because of a decrease in the negative charge of the oxygen. The parallel evolution in the shift of the nonmetallic part of the Al 2p band and that of the O 1s band with increasing titanium deposition time (Figure 4a and 4b), suggests a decrease of the charge transfer from Al to O atoms as a consequence of the formation of cross-linking bonds with Ti atoms. Such a type of cross-linking bonds have been also observed during the oxidation of the Fe/Al and Ni/Al systems[6,7] and also during the first stages of deposition of thin TiO_2 films on SiO_2 and Al_2O_3 substrates.[32,33]

Complementary information on the composition of the oxide film formed can be obtained from the ARXPS results in Figure 7. These results show that the in-depth distribution of species is consistent with the sequence $Al^{ox}-Ti^{4+}$ mixed layer, titanium suboxides ($Ti^{1+} + Ti^{2+} + Ti^{3+}$), and substrate when going from the outer surface to the substrate. For $t \leq 10$ min, the Al^{3+} species seems to be located nearer the surface than the Al^{2+} species, suggesting that Ti−O−Al cross-linking bonds are mainly formed at the interface between $Al^{ox}-Ti^{4+}$ mixed layer and titanium suboxides. This model is idealized, and in reality concentration gradients are to be expected in the layers. The sequential formation of titanium suboxides → Al^{2+} → $Al^{3+}-Ti^{4+}$, in Figure 5a, and titanium suboxides → $Al^{2+}-Ti^{4+}$ in Figure 5b, as the oxygen exposure increases, supports the above-proposed model.

No comparable results exist in the literature on the oxidation of Ti/Al interfaces. However, Mencer et al.[14] using grazing angle XPS measurements to study the oxidation of Ti−Al alloys at temperatures in the 300−873 K range found an increase of the aluminum oxide signal relative to titanium in the near surface. Furthermore, the higher titanium oxidation states were located nearer to the surface than the lower titanium oxidation states. On the other hand, Geng et al.[15] have shown that oxidation of TiAl bulk alloys leads to a multilayered scale, comprising TiO_2 and Al_2O_3, that depends on temperature and oxygen exposure.

Conclusions

The oxidation of titanium deposited on polycrystalline aluminum surfaces has been studied at room temperature and low oxygen pressures, using AES, XPS, and ARXPS. The growth of titanium on the aluminum surfaces occurs in two

stages: formation of a uniform $TiAl_x$ layer up to ~4 ML, followed by the formation of 10 ML thick metallic Ti islands that grow laterally over the $TiAl_x$ layer previously formed. The formation of an aluminum intermediate oxidation state, Al^{2+}, in addition to Al^{3+}, has been observed during the oxidation of Ti/Al interfaces. This intermediate oxidation state is attributed to the formation of Al−O−Ti cross-linking bonds at the interface between an outer aluminum oxide-Ti^{4+} mixed layer and a layer beneath it composed by a mixture of Ti^{1+}, Ti^{2+}, and Ti^{3+} suboxides. Signals related to stoichiometric Al_2O_3, Al^{3+} and O3, decrease as the Ti deposition time increases because of the thickening of the $TiAl_x$ layer during the first stage of Ti growth and because of the subsequent formation of metallic Ti islands during the second stage. In addition to that, the species related to substoichiometric Al oxide, Al^{2+} and O1, continuously increase until the end of the first stage, therefore indicating that the oxidation kinetics begin to be controlled by oxidation of Ti metallic islands formed during this stage. The analysis of the Ti 2p band shows that Ti oxidized always, independent of the stage of Ti growth. However, for Ti/Al interfaces of the first stage, the ratio $Ti^{4+}/(Ti^{1+} + Ti^{2+} + Ti^{3+})$ at oxygen saturation is lower than the ratio expected for a pure Ti substrate. The lack of the oxygen signal characteristic of pure Ti oxidation, O^{Ti}, along with the growth of a species related to the titanium oxidation in the $TiAl_x$ compound, O2, in the high BE side of the Ti 2p band suggest the formation of an aluminum titanate-like compound during the oxidation of the $TiAl_x$ compound.

Acknowledgment. The authors thank D. Díaz for technical assistance. This work is a part of a research project supported by the Spanish Comisión Interministerial de Ciencia y Tecnología (project MAT99-0830-CO3-02).

References and Notes

(1) Den Daas, H.; Passacantando, M.; Lozzi, L.; Santucci, S.; Picozzi, P. *Surf. Sci.* **1994**, *317*, 295.
(2) Strisland, F.; Raaen, S. *J. Electron Spectrosc. Relat. Phenom.* **1996**, *77*, 25.
(3) Stierle, A.; Zabel, H. *Surf. Sci.* **1997**, *385*, 310.
(4) Takehiro, N.; Yamada, M.; Tanaka, K.; Stensgaard, I. *Surf. Sci.* **1999**, *441*, 199.
(5) Maetaki, A.; Yamamoto, M.; Matsumoto, H.; Kishi, K. *Surf. Sci.* **2000**, *445*, 80.
(6) Palacio, C.; Arranz, A. *J. Phys. Chem. B* **2001**, *105*, 10805.
(7) Arranz, A.; Palacio, C. *Langmuir* **2002**, *18*, 1695.
(8) Kim, W. B.; Choi, S. H.; Lee, J. S. *J. Phys. Chem. B* **2000**, *104*, 8670.
(9) Reddy, B. M.; Chowdhury, B.; Reddy, E. P.; Fernández, A. *Langmuir* **2001**, *17*, 1132.
(10) Anpo, M.; Kawamura, T.; Kodama, S.; Maruya, K.; Onishi, T. *J. Phys. Chem.* **1988**, *92*, 438.
(11) Anderson, C.; Bard, A. J. *J. Phys. Chem. B* **1997**, *101*, 2611.
(12) Leinen, D.; Lassaletta, G.; Fernández, A.; Caballero, A.; González-Elipe, A. R.; Martín, J. M.; Vacher, B. *J. Vac. Sci. Technol., A* **1996**, *14*, 2842.
(13) Stabel, A.; Caballero, A.; Espinos, J. P.; Yubero, F.; Justo, A.; González-Elipe, A. R. *Surf. Coat. Technol.* **1998**, *100−101*, 142.
(14) Mencer, D. E.; Hess, T. R., Jr.; Mebrahtu, T.; Cocke, D. L.; Naugle, D. G. *J. Vac. Sci. Technol., A* **1991**, *9*, 1610.
(15) Geng, J.; Gantner, G.; Oelhafen, P.; Datta, P. K. *Appl. Surf. Sci.* **2000**, *158*, 64.
(16) Shanabarger, M. R. *Appl. Surf. Sci.* **1998**, *134*, 179.
(17) Palacio, C.; Arranz, A. *Surf. Interface Anal.* **1999**, *27*, 871.
(18) Arranz, A.; Palacio, C. *Surf. Interface Anal.* **2000**, *29*, 392.
(19) Palacio, C.; Arranz, A. *J. Phys. Chem. B* **2000**, *104*, 9647.
(20) Valeri, S.; Del Pennino, U.; Lomellini, P.; Sassaroli, P. *Surf. Sci.* **1984**, *145*, 371.
(21) Proctor, A.; Sherwood, E. P. A. *Anal. Chem.* **1982**, *54*, 13.
(22) Fuggle, J. C.; Alvarado, S. F. *Phys. Rev. B* **1980**, *22*, 1615.
(23) Pease, D. M. *Phys. Rev. B* **1991**, *44*, 6708.
(24) *Handbook of X-ray Photoelectron Spectroscopy*; Wagner, C. D., Riggs, W. M., Davis, L. E., Moulder, J. F., Muilenberg, G. E., Eds.; Perkin-Elmer Corporation: Eden Prairie, MN, 1979.
(25) Idriss, H.; Barteau, M. A. *Catal. Lett.* **1994**, *26*, 123 and references therein.
(26) McCafferty, E.; Wightman, J. P. *Appl. Surf. Sci.* **1999**, *143*, 92 and references therein.
(27) Rocker, G.; Göpel, W. *Surf. Sci.* **1987**, *181*, 530.
(28) Arranz, A. Ph.D. Thesis, Universidad Autónoma de Madrid, 1998.
(29) Dake, L. S.; Lad, R. J. *Surf. Sci.* **1993**, *289*, 297.
(30) Lu, H.; Bao, C. L.; Shen, D. H.; Zhang, X. J.; Cui, Y. D.; Lin, Z. D. *J. Mater. Sci.* **1995**, *30*, 339.
(31) Arranz, A.; Palacio, C. *Surf. Sci.* **1996**, *355*, 203.
(32) Lassaletta, G.; Fernández, A.; Espinós, J. P.; González-Elipe, A. R. *J. Phys. Chem.* **1995**, *99*, 1484.
(33) Sánchez-Agudo, M.; Soriano, L.; Quirós, C.; Avila, J.; Sanz, J. M. *Surf. Sci.* **2001**, *482−485*, 470.